



## Benefits of Demand Side Management strategies for an island supplied by marine renewable energies

Anthony Roy, François Auger, Salvy Bourguet, Florian Dupriez-Robin, Quoc Tuan Tran

### ► To cite this version:

Anthony Roy, François Auger, Salvy Bourguet, Florian Dupriez-Robin, Quoc Tuan Tran. Benefits of Demand Side Management strategies for an island supplied by marine renewable energies. 2018 7th IEEE International Conference on Renewable Energy Research and Applications (ICRERA), Oct 2018, Paris, France. pp.474-481, 10.1109/ICRERA.2018.8566784 . hal-02418784

**HAL Id: hal-02418784**

**<https://hal.science/hal-02418784>**

Submitted on 7 Feb 2024

**HAL** is a multi-disciplinary open access archive for the deposit and dissemination of scientific research documents, whether they are published or not. The documents may come from teaching and research institutions in France or abroad, or from public or private research centers.

L'archive ouverte pluridisciplinaire **HAL**, est destinée au dépôt et à la diffusion de documents scientifiques de niveau recherche, publiés ou non, émanant des établissements d'enseignement et de recherche français ou étrangers, des laboratoires publics ou privés.

# Benefits of Demand Side Management strategies for an island supplied by marine renewable energies

Anthony Roy, François Auger,  
Salvy Bourguet  
IREENA, Université de Nantes,  
37 Boulevard de l'Université,  
44600 Saint-Nazaire, France  
anthony.roy1@univ-nantes.fr,  
francois.auger@univ-nantes.fr,  
salvy.bourguet@univ-nantes.fr

Florian Dupriez-Robin  
CEA Tech Pays de la Loire  
Technocampus Océan,  
5 Rue de l'Halbrane,  
44340 Bouguenais, France  
florian.dupriez-robin@cea.fr

Quoc Tuan Tran  
CEA-LITEN,  
50 Av. du Lac Léman,  
73370 Le Bourget-du-Lac, France  
quoctuan.tran@cea.fr

**Abstract** — While marine renewable energies have seen some interest over the last years, the electricity supply of maritime remote areas still presents many constraints, such as high costs due to the storage requirements. The constraints related to the reliance show that the energy management system needs some flexibility, which can be done by managing the demand. The strategies based on load shed and load postponement are often considered. In this paper, anticipation based strategies are proposed in the aim to use the excess power for shiftable loads supply and to foster marine energies integration for the electricity supply of remote areas. A multi-source system including solar, wind, tidal and wave energies is considered, in which batteries are used to ensure the demand to be satisfied as much as possible. The developed strategies concern the electric room heaters and water heaters power demand. Significant effects on demand satisfaction, battery lifetime, system sizing and costs are observed in the carried out simulations, showing the positive effects brought by the proposed anticipation based strategies. Moreover, some situations of loss of power supply are avoided thanks to the proposed demand side management strategies.

**Keywords** — *Marine renewable energies, Demand Side Management strategies, load shifting, off-grid, island electricity supply*

## I. INTRODUCTION

In maritime remote areas, electricity supply is mostly provided by solar and wind energies [1, 2]. Batteries and gensets are often used to ensure the demand to be met in case of low generation [3, 4]. In addition to the pollution generated by the use of gensets, fuel import is sometimes costly, because of logistical constraints in remote areas [1]. Avoiding the use of gensets leads to more constraints on reliability, sizing and costs for a system based on renewable energies and batteries. Moreover, the variable nature of renewable energies can lead to situations where demand cannot be fully met. So as to avoid the installation of an under-utilized generation capacity or a high storage capacity, the energy management system needs some flexibility. Demand Side Management (DSM) strategies can help to change the shape of the load curve according to the available generated power [5]. The main DSM strategies found in the literature are classified in six categories: peak clipping,

valley filling, load shifting, strategic load growth, strategic load conservation and flexible load shape [6, 7]. Strategies based on load shifting for which delay and advance scheduling can be considered [8, 9] are the most used [7, 10, 11, 12]. They allow the demanded energy to be conserved, which is not the case with the peak clipping strategy, where load is shed [13]. Among all the flexible loads which can be considered, the water heaters and the electric room heaters are often studied in papers dealing with DSM [14, 15]. A review of DSM schemes and programs is given in [5], according to the possible control mechanisms and the motivations offered to consumers in order to participate to the load management program. Some programs consist in time-varying pricing, whereas others are based on incentive offers. In addition to the desired reliability benefits, DSM could bring technical, economic, environmental and social benefits, as described in [10, 16, 17]. The application of DSM strategies can also allow the storage capacity to be reduced [18], leading to a cost reduction. While marine renewable energies present high costs [19], DSM could help to reduce the costs of electricity supply in remote areas, as shown in a recent study [20] dealing with a multi-source system based on solar, wind and wave energies. So as to foster the integration of renewable energies available in maritime areas, such as solar, wind, tidal and wave energies, and to bring flexibility to the energy management strategies, DSM strategies are developed in this work. Anticipation strategies are simulated for water heaters and electric room heaters loads, instead of delay shifting strategies usually applied. Section 2 describes the considered multi-source system, the load profile separation and the economic and reliability evaluation method. The developed DSM strategies are presented in Section 3, resulting in several benefits summarized in Section 4.

## II. MULTI-SOURCE SYSTEM DESCRIPTION AND MODELING

The offgrid multi-source system considered in this paper is based on solar, wind, tidal kinetic and wave energies. At each time sample  $t_k$ , the total generated power  $P_{gen}$  corresponds to the sum of powers generated by the four sources:

$$P_{gen}(t_k) = N_{PV} \times P_{PV}(t_k) + N_{WT} \times P_{e,w}(t_k) + N_{TT} \times P_{e,t}(t_k) + N_{WEC} \times P_{WEC}(t_k) \quad (1)$$

where  $N_{PV}$  is the number of PV panels,  $P_{PV}$  is the photovoltaic panel output power [W],  $N_{WT}$  is the number of wind turbines,  $P_{e,w}$  is the wind turbine electrical output power [W],  $N_{TT}$  is the number of tidal turbines,  $P_{e,t}$  is the tidal turbine electrical output power [W],  $P_{WEC}$  is the wave energy converter output electrical power and  $N_{WEC}$  is the number of wave energy converters.

In order to ensure the requested power be met in case of low production, lithium-ion batteries are added to the multi-source system. The case study of this paper concerns the Ouessant Island (located on the west coast of France), as the tidal kinetic and the wave resources reach a sufficiently high level to consider their exploitation. The availability of both resource and load profile data allows to conduct simulations for a five years long period at hourly time step, from January 1<sup>st</sup> 2011 to December 31<sup>st</sup> 2015. This section summarizes the used models and describes the reliance and costs models. An overview of the considered system is given in Fig. 1.

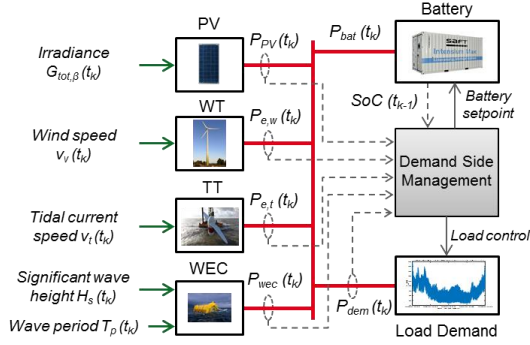


Fig. 1. Overview of the considered multi-source system model

#### A. Photovoltaic panel model

Considering the use of a MPPT control (Maximum Power Point Tracking), the photovoltaic panel output power  $P_{PV}$  is calculated according to [21]:

$$P_{PV} = \eta_{PV} \times S_{PV} \times G_{tot,\beta} \quad (2)$$

where  $S_{PV}$  the panel area [m<sup>2</sup>],  $G_{tot,\beta}$  the global irradiance [W/m<sup>2</sup>] received by the tilted surface ( $\beta$  is the tilt angle) and  $\eta_{PV}$  is the module efficiency, which depends on the cell temperature  $T_c$ :

$$\eta_{PV} = \eta_{PV,ref} \times \eta_{conv,PV} \times [1 + \alpha_p \times (T_c - T_{c,ref})] \quad (3)$$

$$T_c = T_{amb} + (T_{c,NOCT} - T_{amb,NOCT}) \times \frac{G_{tot,\beta}}{G_{NOCT}} \quad (4)$$

where  $\eta_{PV,ref}$  is the module efficiency in Standard Test Conditions (STC),  $\eta_{conv,PV}$  the conversion chain efficiency,  $\alpha_p$  the temperature coefficient [°C<sup>-1</sup>],  $T_c$  the cell temperature [°C],  $T_{c,ref}$  the STC cell temperature [°C] and  $T_{amb}$  the air temperature [°C].  $T_{c,NOCT}$  is the cell temperature [°C],  $T_{amb,NOCT}$  is the air temperature [°C] and  $G_{NOCT}$  is the irradiance [W/m<sup>2</sup>] under Nominal Operating Cell Temperature conditions (NOCT).

The photovoltaic panel considered in this paper is the SX3195 reference from BP Solar manufacturer with  $P_{r,PV} = 190$  W (the PV panel rated power),  $S_{PV} = 1.411$  m<sup>2</sup>,  $\eta_{PV,ref} = 0.135$ ,  $\eta_{conv} = 0.95$ ,  $\alpha_p = -0.0048$  °C<sup>-1</sup>,  $T_{c,ref} = 25$  °C,  $T_{c,NOCT} = 47$  °C,  $T_{amb,NOCT} = 20$  °C and  $G_{NOCT} = 800$  W/m<sup>2</sup>. The PV panel is facing south, considering a tilt angle  $\beta$  about 40°. Irradiance data used in this paper come from CAMS database (Copernicus Atmosphere Monitoring Service Information) [22] and air temperature data are provided by OpenOcean SAS [23].

#### B. Wind turbine model

The wind turbine output power  $P_{e,w}$  is deduced from the power curve interpolation of the considered turbine [24], depending on the wind speed value  $v_w$ . For the second zone of the power curve, the power characteristic is interpolated by a 5th order polynomial approximation:

$$P_{e,w}(v_w) = \begin{cases} 0 & , v_w < v_{w,cut-in} \\ \sum_{i=0}^5 a_i v_w^i & , v_{w,cut-in} \leq v_w \leq v_{w,r} \\ P_{r,WT} & , v_{w,r} < v_w \leq v_{w,cut-out} \\ 0 & , v_{w,cut-out} < v_w \end{cases} \quad (5)$$

Where  $P_{r,WT}$  the wind turbine nominal power [W],  $v_w$  the wind speed [m/s],  $v_{w,cut-in}$  the cut-in speed,  $v_{w,r}$  the rated speed,  $v_{w,cut-out}$  the cut-out speed and  $a_i$  the polynomial approximation coefficients (5<sup>th</sup> order).

In this paper, the E-53/800 wind turbine system from Enercon is considered, according to the power curve available in [25]. The main characteristics of this wind turbine are:  $P_{r,WT} = 810$  kW,  $v_{w,cut-in} = 3$  m/s,  $v_{w,r} = 13$  m/s and  $v_{w,cut-out} = 25$  m/s. The wind speed data used in this paper are also provided by OpenOcean SAS.

#### C. Tidal turbine model

A marine current turbine is considered in the multi-source system, extracting the tidal current kinetic energy. The tidal turbine electrical output power  $P_{e,t}$  depends on the tidal velocity thresholds of the power curve [26]:

$$P_{e,t}(v_t) = \begin{cases} 0 & , v_t < v_{t,cut-in} \\ 0.5 C_{p,t} \rho_w S v_t^3 \eta_{conv,TT} & , v_{t,cut-in} \leq v_t \leq v_{t,r} \\ P_{r,TT} & , v_{t,r} < v_t \leq v_{t,cut-out} \\ 0 & , v_{t,cut-out} < v_t \end{cases} \quad (6)$$

where  $P_{r,TT}$  the tidal turbine nominal power [W],  $v_t$  the tidal current velocity [m/s],  $v_{t,cut-in}$  the cut-in velocity,  $v_{t,r}$  the rated velocity,  $v_{t,cut-out}$  the cut-out velocity,  $C_{p,t}$  the tidal turbine power coefficient,  $\rho_w$  the sea water density (1024 kg/m<sup>3</sup>),  $S$  the area swept by the tidal turbine blades [m<sup>2</sup>] and  $\eta_{conv,TT}$  the conversion chain efficiency.

The T500 tidal turbine from Tocardo is considered in this paper, with  $P_{r,TT} = 300$  kW,  $v_{t,cut-in} = 0.5$  m/s,  $v_{t,r} = 2.5$  m/s,  $v_{t,cut-out} = 3.8$  m/s,  $C_{p,t} = 0.359$ ,  $S = 104.2$  m<sup>2</sup> and  $\eta_{conv,TT} = 0.85$ . The tidal current data used in this paper are

extracted from the FINIS250 database produced within the scope of the Previmer program [27].

#### D. Wave energy converter model

The wave energy converter output electrical power  $P_{WEC}$  is computed by interpolating a power matrix, according to the sea state parameters (the significant wave height  $H_s$  and the energetic period  $T_e$ ). The Oyster wave energy converter is considered in this paper, with the corresponding power matrix presented in Table 1 [28] for which  $P_{WEC}$  is given in kilowatts (the nominal power is  $P_{r,WEC} = 290$  kW). Wave data used in this paper are based on the WaveWatchIII model [29].

TABLE I. OYSTER WEC POWER MATRIX

$T_e$ (s) → $H_s$ (m)	5	6	7	8	9	10	11	12	13
0.5	0	0	0	0	0	0	1	3	3
1	20	30	38	42	44	44	45	47	45
1.5	80	85	92	97	102	103	104	100	104
2	140	147	152	158	155	155	160	161	156
2.5	192	197	208	202	203	209	211	201	204
3	241	237	237	241	243	230	236	231	235
3.5	0	271	272	269	268	267	270	260	260
4	0	291	290	290	280	287	276	278	277
4.5	0	291	290	290	280	287	276	278	277
5	0	0	290	290	280	287	276	278	277
5.5	0	0	290	290	280	287	276	278	277
6	0	0	290	290	280	287	276	278	277

#### E. Battery model

Lithium-ion batteries are added to the multi-source system to ensure the load requirements to be met in case of low generation. Two models of the State of Charge (SoC) and of the State of Health (SoH) are considered [30, 31]. The SoC value is get at each time sample  $t_k$  according to the battery set point power  $P_{bat}(t_k)$  [30] by

$$SoC(t_k) = SoC(t_{k-1}) \times (1 - \sigma)^{\frac{\Delta t}{24}} + \frac{P_{bat}(t_k) \times \Delta t \times \eta_{bat}}{C_{bat ref}} \quad (7)$$

$$P_{bat}(t_k) = \frac{P_{gen}(t_k) - P_{dem}(t_k)}{N_{bat}} \quad (8)$$

Where  $C_{bat ref}$  is the battery nominal capacity [Wh],  $N_{bat}$  the battery number,  $P_{bat}$  the battery power [W] (negative during discharge and positive during charge),  $P_{dem}$  the load demand power [W],  $\Delta t$  the time step [h],  $\sigma$  the daily self-discharge rate and  $\eta_{bat}$  the battery efficiency.

Battery is charged if the total generated power is larger than the demand power, and discharged otherwise. Battery charge and discharge are constrained by SoC and power limits:

$$SoC_{min} < SoC(t_k) < SoC_{max} \quad (9)$$

$$P_{disch max} < P_{bat}(t_k) < P_{ch max} \quad (10)$$

Battery ageing is calculated at each time sample by the evaluation of the State of Health (SoH), according to the lifetime maximum exchanged energy method described in [31]:

$$SoH(t_k) = SoH(t_{k-1}) - \frac{|P_{bat}(t_k)| \times \Delta t}{E_{exch max}} \quad (11)$$

$$E_{exch max} = 2 \times C_{bat ref} \times DoD \times N_{cycles max}(DoD) \quad (12)$$

where  $SoH$  is the battery state of health,  $E_{exch max}$  the maximum energy which can be exchanged during battery lifetime [Wh],  $DoD$  the depth of discharge,  $N_{cycles max}$  the maximum cycle number according to the considered  $DoD$ .

The battery considered in this study is the Max+20M from Saft, with:  $C_{bat ref} = 1.09$  MWh,  $P_{ch max} = 2.2$  MW,  $P_{disch max} = -2.5$  MW,  $\sigma = 0.166$  %/day and  $\eta_{bat} = 0.96$ . Battery replacement is considered when  $SoH = 0.7$ , with  $SoC_{min} = 0.1$ ,  $SoC_{max} = 0.95$ ,  $E_{exch max} = 6.485$  MWh,  $N_{cycles max} = 3500$  cycles for  $DoD = 0.9$ .

#### F. Load profile model

The load profile data considered in this paper are provided by EDF SEI [32], corresponding to the Ouessant Island hourly load demand. The energy consumed each year is about 6 GWh, with a 2 MW peak load power in winter. Electricity demand of this island is mostly attributed to domestic needs [33]. Indeed, the annual energy consumed by the residential sector amounts to 70% of the total energy. The other part is related to the tertiary sector, such as restaurants and shops, as the economic activity of the island is mostly related to tourism. According to the information available in [32, 33] and the following hypotheses, a load profile separation is carried out to get the following three load profiles:

- *Electric room heaters*: a thermo-sensibility analysis is conducted according to the method proposed in [34]. A linear regression is performed on the daily energy demand curve according to the daily average air temperature. A 15°C daily average air temperature threshold is considered for the electric room heater turn off. Annual energy related to electric heaters amounts to 51.1 % of the total annual energy of the Ouessant Island. The power  $P_{HT}$  related to electric room heaters is considered as a constant during the whole day.
- *Water heaters*: profile extraction is based on electricity tariff policy applied in France, following a nightly operation cycle. Thus, water heaters operate for eight hours at night (between 21 p.m. and 5 a.m.), i.e. during the low price policy period. Annual energy attributed to the water heaters amounts to 5.6 % of the total annual energy. Although a peak is usually observed at turn on [14], the power related to water heater  $P_{WH}$  is considered as a constant during these eight hours. Indeed, a profusion of consumptions must be considered, allowing the load profile related to water heater demand to be smoothed.
- *Non-shiftable loads*: as little information is available, no others kinds of loads are considered for DSM strategies. Thus, the non-shiftable power consumption  $P_{NS}$  corresponds to the remaining load profile.

Thus, at each time sample, the total requested power  $P_{dem}$  can be defined as:

$$P_{dem}(t_k) = P_{HT}(t_k) + P_{WH}(t_k) + P_{NS}(t_k) \quad (13)$$

Examples of three days long load profiles in winter and in summer are given in Fig. 2.

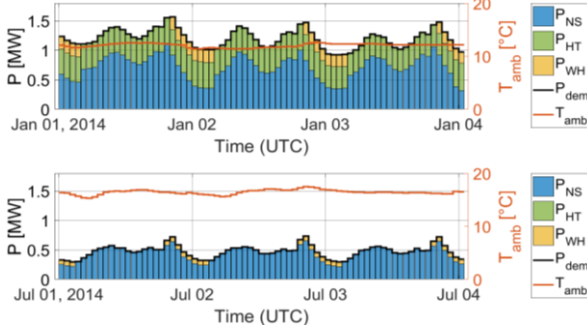


Fig. 2. Examples of winter (top) and summer (bottom) load profiles and the corresponding hourly air temperature measurement

### G. Reliability and costs evaluation

The multi-source system considered in this paper is evaluated according to two criteria. The first criterion is related to the reliance aspect. The unmet load demand is evaluated according to the LPSP (*Loss of Power Supply Probability*) [21], given by:

$$LPSP = \frac{E_{loss}}{E_{dem}} \quad (14)$$

Where  $E_{dem}$  is the demanded energy during the simulated period [Wh] and  $E_{loss}$  is the demanded energy which cannot be supplied by the sources and the battery [Wh].

The second criterion is related to the economic evaluation, thanks to Levelized Cost Of Energy ( $LCOE$ ) [€/kWh], based on the Life Cycle Cost ( $LCC$ ) [€] and the system lifetime demanded energy  $E_{dem,N}$  [Wh], according to the method given in [19]:

$$LCOE = \frac{LCC}{E_{dem,N}} = \frac{(\sum_{i=1}^4 LCC_{S,i}) + LCC_{ESS}}{E_{dem,N}} \quad (15)$$

For each source  $i$  of the considered multi-source system, the life cycle cost calculation includes investment costs ( $C_{inv,i}$ ) and operation and maintenance costs ( $C_{O\&M,i}$ ):

$$LCC_{S,i} = C_{inv,i} + C_{O\&M,i} = C'_{inv,i} \times P_{inst,i} + \sum_{t=1}^N \frac{C'_{O\&M,i} \times P_{inst,i}}{(1+r_i)^t} \quad (16)$$

Where  $LCC$  is the Life Cycle Cost [€],  $C'_{inv,i}$  is the unitary investment cost [€/kW],  $P_{inst,i}$  the installed power [kW],  $C'_{O\&M,i}$  the annual operation and maintenance costs [€/kW/year],  $N$  the system lifetime [years],  $r_i$  the interest rate [%] and  $t$  the considered year, from the beginning of the project to the  $N$ -th year. The sources lifetime is considered to be the same as the system lifetime ( $N = 25$  years).

The economic parameters related to the sources are given in Table II, according to data available in [19, 35].

TABLE II. SOURCES ECONOMIC PARAMETERS

Source	Economic parameter		
	Investment costs $C'_{inv}$	O&M costs $C'_{O\&M}$	Interest rate $r$
PV	1600 €/kW	48 €/kW	5 %
WT	1350 €/kW	47 €/kW	5 %
TT	6800 €/kW	250 €/kW	5 %
WEC	3700 €/kW	230 €/kW	5 %

The battery life cycle cost  $LCC_{ESS}$  includes investment costs  $C_{inv,ESS}$ , operation and maintenance (O&M) costs  $C_{O\&M,ESS}$  and replacement cost  $C_{r,ESS}$  [36], according to:

$$LCC_{ESS} = C_{inv,ESS} + C_{O\&M,ESS} + C_{r,ESS} \quad (17)$$

$$C_{inv,ESS} = C'_{inv,ESS} \times E_{inst,ESS} \quad (18)$$

$$C_{O\&M,ESS} = \sum_{t=1}^N \frac{\alpha_{O\&M,ESS} \times C_{inv,ESS}}{(1+r_{ESS})^t} \quad (19)$$

$$C_{r,ESS} = N \times CRF \times \sum_{k=1}^{n_r} \frac{C_{inv,ESS}}{(1+r_{ESS})^{k \times t_{l,ESS}}} \quad (20)$$

$$CRF = \frac{r_{ESS} \times (1+r_{ESS})^N}{(1+r_{ESS})^N - 1} \quad (21)$$

Where  $C'_{inv,ESS}$  is the unitary investment cost [€/kWh],  $E_{inst,ESS}$  the battery storage capacity [kWh],  $\alpha_{O\&M,ESS}$  the part of investment cost corresponding to O&M costs,  $r_{ESS}$  the interest rate,  $CRF$  the capital recovery factor,  $n_r$  the battery replacement occurrences during the system exploitation duration and  $t_{l,ESS}$  the battery lifetime [years]. The parameters related to the lithium-ion battery costs are based on [37, 38], with  $C'_{inv,ESS} = 860$  €/kWh,  $\alpha_{O\&M,ESS} = 0.02$  and  $r_{ESS} = 5\%$ .

### III. DESIGNED DEMAND SIDE MANAGEMENT STRATEGIES

Two kinds of loads are considered for DSM strategies: water heaters and electric room heaters. Among all the possible DSM strategies, only time shift based strategies are applied in our work, by anticipating totally or partially the water heaters and/or electric room heaters demand initially planned at a given time sample. No postponement strategy is considered in this paper. Generally speaking, the proposed load shifting strategies can be considered only if the following two conditions are satisfied:

- The battery must be fully charged, according to the previous iteration  $SoC$  value:

$$SoC(t_{k-1}) = SoC_{max} \quad (22)$$

- The generated power  $P_{gen}$  must be larger than the demanded power  $P_{dem}$  at  $t_k$ . Thus, the resulting excess of generated power  $P_{exc}$  is defined as:

$$P_{exc}(t_k) = \begin{cases} P_{gen}(t_k) - P_{dem}(t_k), & \text{if } P_{gen}(t_k) > P_{dem}(t_k) \\ 0, & \text{otherwise} \end{cases} \quad (23)$$

The powers related to the water heaters and the electric room heaters after DSM strategies application will be respectively noted  $P'_{WH}$  and  $P'_{HT}$ . Thus, at each time sample, the total load power  $P'_{dem}$  after DSM strategies application is defined as:

$$P'_{dem}(t_k) = P'_{HT}(t_k) + P'_{WH}(t_k) + P_{NS}(t_k) \quad (24)$$

More specific conditions for both loads are considered, which are detailed in the following subsections.

#### A. Water heaters strategy

An anticipation load shifting strategy is considered for water heaters management. If, at a time sample  $t_k$ , the generated power is larger than the demand and if the batteries are fully charged, the next water heaters operating occurrence initially planned at  $t_{k+A}$  is shifted at  $t_k$ , whatever the power amount generated at  $t_{k+A}$ . Anticipation may start ten hours before the originally planned period ( $1 \leq A \leq 10$ ). An overview of the data related to the proposed strategy is given in Fig. 3. The data related to the next ten hours of water heaters load profile and the excess power at  $t_k$  are needed to evaluate the proposed strategy.

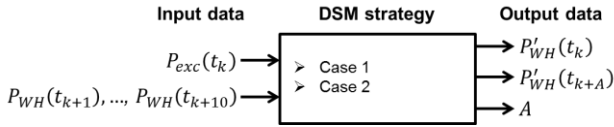


Fig. 3. Overview of the data related to the water heaters DSM strategy

The anticipated consumption is constrained by the excess power  $P_{exc}$  at  $t_k$ , defined by (23). Thus, two cases can be found:

- Case 1: if  $P_{exc}(t_k) \geq P_{WH}(t_{k+A})$ , the water heaters demand is totally shifted from  $t_{k+A}$  to  $t_k$  as the excess power is large, resulting in:

$$P'_{WH}(t_k) = P_{WH}(t_{k+A}) \quad (25)$$

$$P'_{WH}(t_{k+A}) = 0 \quad (26)$$

- Case 2: if  $P_{exc}(t_k) < P_{WH}(t_{k+A})$ , the water heaters demand is partially shifted from  $t_{k+A}$  to  $t_k$  as the excess power is low, resulting in:

$$P'_{WH}(t_k) = P_{exc}(t_k) \quad (27)$$

$$P'_{WH}(t_{k+A}) = P_{WH}(t_{k+A}) - P_{exc}(t_k) \quad (28)$$

In case 1, all the water heaters are concerned by the anticipated turn on, whereas in case 2 only some water heaters are concerned (the quantity is defined according to the amount of excess power). The anticipated consumption cannot overpass the initially planned water heaters power. An overview of the developed DSM strategy for water heaters is

given in Fig. 4, showing a totally and a partially anticipated consumption.

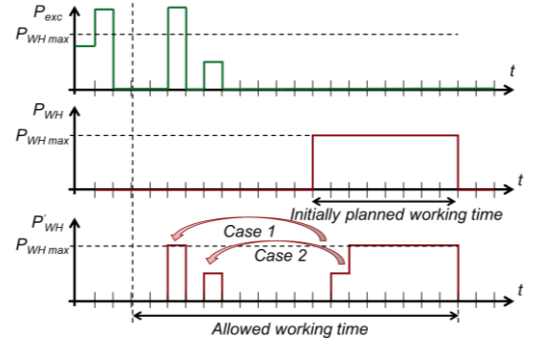


Fig. 4. Working principle of the proposed water heaters DSM strategy (case 1 represents a totally shifted consumption, whereas case 2 shows a partially consumption anticipation)

#### B. Electric room heaters strategy

Anticipation is also considered for electric room heaters in case of excess production at time  $t_k$ , but with a shorter time window and only in case of subsequent deficiency. The electric heaters load planned at a future time sample  $t_{k+B}$  is anticipated only if a lack of power at  $t_{k+B}$  exists, defined by:

$$P_{def}(t_{k+B}) = \begin{cases} P_{dem}(t_{k+B}) - P_{gen}(t_{k+B}), & \text{if } P_{gen}(t_{k+B}) < P_{dem}(t_{k+B}) \\ 0, & \text{otherwise} \end{cases} \quad (29)$$

Anticipation time is limited to two hours ( $B = 1$  or  $2$ ) and the anticipated consumption is constrained by the available power  $P_{exc}$  at  $t_k$  and by the lack of power  $P_{def}$  at  $t_{k+B}$ , to limit the discomfort brought by this DSM strategy. An overview of the data related to the proposed strategy is given in Fig. 5. To apply the designed strategy, a two hours forecasting ability is considered in this strategy to evaluate the lack of power  $P_{def}$  at  $t_{k+B}$ . Moreover, the power related to electric heaters for the next two hours and the excess of power at  $t_k$  are needed.



Fig. 5. Overview of the data related to the electric room heaters DSM strategy

According to the  $P_{exc}(t_k)$  and  $P_{def}(t_{k+B})$  values, four cases are possible, implying the application of one of the following rules, firstly for  $B = 1$  then for  $B = 2$ .

At  $t_{k+B}$ , if the lack of power is higher than the electric room heaters demand ( $P_{def}(t_{k+B}) \geq P_{HT}(t_{k+B})$ ), the electric room heaters load is anticipated as much as possible, according to the available power at  $t_k$  and the electric heaters demand at  $t_{k+B}$ :

- Case 1: if  $P_{exc}(t_k) \geq P_{HT}(t_{k+B})$ ,

$$P'_{HT}(t_k) = P_{HT}(t_k) + P_{HT}(t_{k+B}) \quad (30)$$



$$P'_{HT}(t_{k+B}) = 0 \quad (31)$$

- Case 2: if  $P_{exc}(t_k) < P_{HT}(t_{k+B})$ ,

$$P'_{HT}(t_k) = P_{HT}(t_k) + P_{exc}(t_k) \quad (32)$$

$$P'_{HT}(t_{k+B}) = P_{HT}(t_{k+B}) - P_{exc}(t_k) \quad (33)$$

Otherwise, if at  $t_{k+B}$  the lack of power is lower than the electric heaters demand ( $P_{def}(t_{k+B}) < P_{HT}(t_{k+B})$ ), only a part of electric room heaters power is anticipated, according to the available power at  $t_k$  and the lack of power at  $t_{k+B}$ :

- Case 3: if  $P_{exc}(t_k) \geq P_{def}(t_{k+B})$ ,

$$P'_{HT}(t_k) = P_{HT}(t_k) + P_{def}(t_{k+B}) \quad (34)$$

$$P'_{HT}(t_{k+B}) = P_{HT}(t_{k+B}) - P_{def}(t_{k+B}) \quad (35)$$

- Case 4: if  $P_{exc}(t_k) < P_{def}(t_{k+B})$ ,

$$P'_{HT}(t_k) = P_{HT}(t_k) + P_{exc}(t_k) \quad (36)$$

$$P'_{HT}(t_{k+B}) = P_{HT}(t_{k+B}) - P_{exc}(t_k) \quad (37)$$

The amount of anticipated consumption would correspond to a temperature set point modulation.

#### IV. SIMULATION RESULTS AND DISCUSSION

The designed DSM strategies are included into the simulation flowchart of the multi-source system, proposed in Fig. 6. Simulations are carried out over a five years long period at hourly time step according to different configurations. In order to show the consequences and the benefits brought by each anticipation based DSM strategy, the proposed strategies are applied separately, firstly on water heaters demand then on electric room heaters. Finally, both DSM strategies are applied simultaneously. Simulations are carried out considering the following multi-source system sizing:  $N_{PV} = 1500$ ,  $N_{WT} = 6$ ,  $N_{TT} = 6$ ,  $N_{WEC} = 3$  and  $N_{bat} = 7$ . Some examples of load profiles without and with DSM strategies are proposed in Fig. 7-10 (only a period starting on 02/17/2015 at 9:00 a.m. and ending on 02/18/2015 at 12:00 a.m. is displayed).

Fig. 8-10 shows that the anticipation of water heaters and/or electric room heaters demand allows the battery discharge to be reduced, as the SoC remains at a value over 0.7 whereas the SoC value reaches 0.6 without DSM strategy application. During this period, it can be observed that water heaters demand is shifted to the diurnal hours (Fig. 8), corresponding to the case 2 described in the proposed water heaters DSM strategy. Moreover, the electric room heaters consumption is anticipated two times as shown in Fig. 9 (the case 2 described in the proposed methodology is observed for the Feb. 17<sup>th</sup>, 19:00 occurrence, whereas the case 4 is observed for the Feb. 18<sup>th</sup>, 8:00 occurrence).

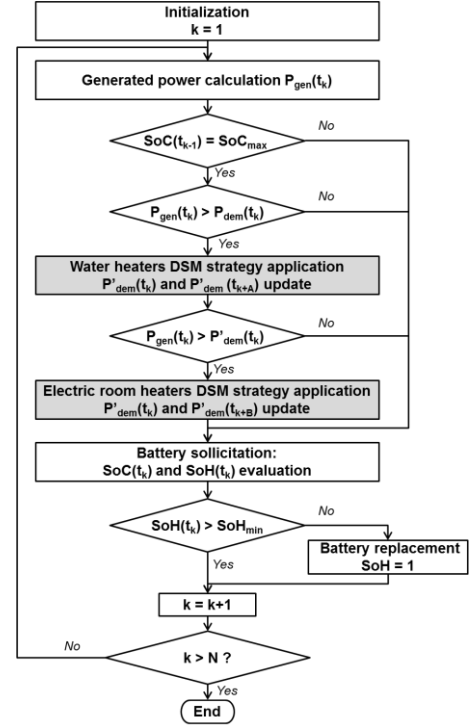


Fig. 6. General flowchart of the multi-source system simulation, including DSM strategies

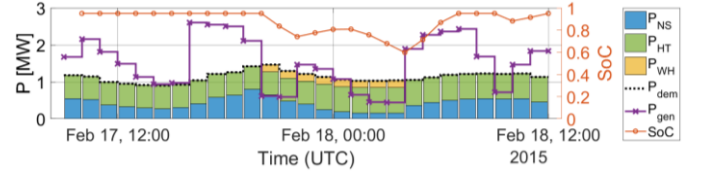


Fig. 7. Simulation without DSM

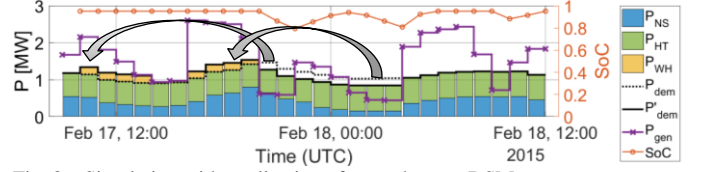


Fig. 8. Simulation with application of water heaters DSM strategy

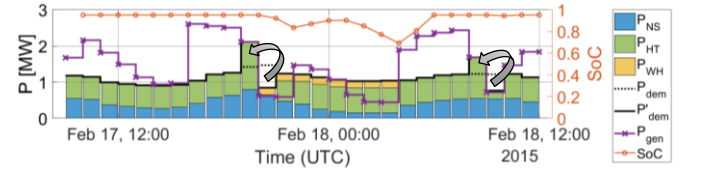


Fig. 9. Simulation with application of electric room heaters DSM strategy

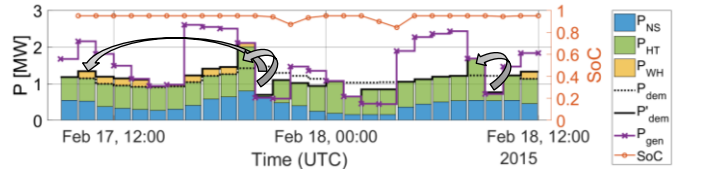


Fig. 10. Simulation with application of water heaters and electric room heaters DSM strategies

Moreover, the simulation results over the five years long period show several positive effects on different criteria. The following observations can be done according to the results summarized in Table III:

- Unmet load: according to the LPSP and the unmet load hours evaluation, the unmet demand is reduced, especially when the water heater DSM strategy is applied. However, the proposed DSM strategies applied to the considered multi-source system sizing cannot avoid hours of unmet demand.
- Battery lifetime: by using the excess of generated power to supply shiftable loads, the battery use is avoided thus the *SoH* degradation is slowed down, allowing the battery lifetime to be extended by a few years.
- Required battery quantity to ensure the demand to be fully satisfied: the number of batteries required is reduced with application of the proposed DSM strategies.
- Levelized Cost Of Energy: as the number of batteries can be reduced by applying the proposed DSM strategies, a reduction of LCOE can be observed, although it is limited since the resulting cost reduction is about -1.6%.

TABLE III. DSM STRATEGIES APPLICATION RESULTS

Strategy Criteria	Without DSM	Water heaters DSM	Electric heaters DSM	Water Heaters + Electric heaters DSM
Unmet load hours [h]	161	144	155	<b>138</b>
LPSP [%]	0.277	0.252 (- 8.8 %)	0.269 (- 2.9 %)	<b>0.245</b> (- 11.5 %)
Energy supplied by the battery [GWh]	1.12	1.02 (- 8.4 %)	1.01 (- 9.4 %)	<b>0.94</b> (- 16.5 %)
Battery lifetime [years]	30.3	33.1 (+ 9.3 %)	33.4 (+10.7 %)	<b>36.2</b> (+19.7 %)
Number of battery required	34	33	33	<b>33</b>
LCOE [€/kWh]	0.466	0.458 (- 1.6 %)	0.458 (- 1.6 %)	<b>0.458</b> (- 1.6 %)
Life Cycle Cost (LCC) [M€]	75.93 (- 1.6 %)	74.73 (- 1.6 %)	74.73 (- 1.6 %)	<b>74.73</b> (- 1.6 %)

By evaluating the load factor  $LF$  for each source at each time sample, defined as the ratio between the generated power and the installed power, a trend between the demand modification and the power generated by some sources can be observed. Table IV presents the average load factor of each source, evaluated for the occurrences for which the water heaters demand or the electric room heaters demand have been increased or reduced. Generally, it appears, according to Table IV, that the water heaters demand is shifted to periods for which the photovoltaic panels load factor is large (during the day), whereas electric room heaters demand is shifted to periods for which tidal turbines load factor is large, according to the infra-day cycles of tidal currents. Regarding the period shown in Fig. 8 and the evaluation of the hourly load factor for each sources given in Fig. 9, it appears that the water heaters consumption has been shifted to occurrences where PV and

tidal turbine load factors are large, whereas electric room heaters have been anticipated to occurrences where the tidal turbines load factor is large. It can be noted that a strategy consisting to systematically shift the operating working time of water heaters during the diurnal hours (during the maximum PV load factor), would not be as interesting as the proposed strategy. Indeed, this strategy would not consider the amount of excess power, which can be low or zero in case of cloudy day, whereas the strategy proposed in this paper allows the load shifting to be applied only if an excess exists.

TABLE IV. MEAN LOAD FACTORS FOR LOAD MODIFICATION OCCURRENCES

Considered occurrences $t_k$ for $LF$ evaluation	$LF_{PV}$	$LF_{WT}$	$LF_{TT}$	$LF_{WEC}$
$P'_{WH}(t_k) < P_{WH}(t_k)$	<b>0</b>	0.547	0.364	0.273
$P'_{WH}(t_k) > P_{WH}(t_k)$	<b>0.356</b>	0.5890	0.359	0.275
$P'_{HT}(t_k) < P_{HT}(t_k)$	0.118	0.047	<b>0.059</b>	0.13
$P'_{HT}(t_k) > P_{HT}(t_k)$	0.129	0.072	<b>0.339</b>	0.159

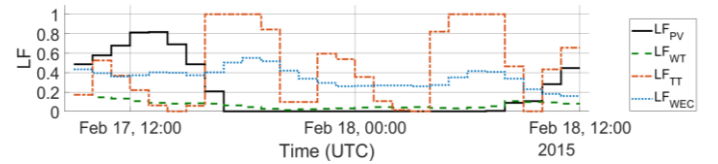


Fig. 11. Hourly load factor of each source

## V. CONCLUSION

The proposed strategies based on the anticipation of water heaters and electric room heaters allow the load satisfaction to be improved and the battery lifetime to be lengthened. Unlike strategies based on load delay, the anticipation based strategies present a lower discomfort for the user and reduce loss of power supply situations. By applying the proposed strategies, the excess power is used for shiftable loads supply. Thus, the proposed DSM strategies allow the reliance of a marine energies based multi-source systems to be improved. By using the solar irradiance and the tidal currents resources which present predictable cycles, the water heaters demand could be scheduled according to these cycles. Also, the fluctuations of power generated by a tidal turbine bring some possibilities for electric heating management while limiting the discomfort for the user.

## ACKNOWLEDGMENT

This work was supported by the project "Monitoring and management of marine renewable energies" granted by the "Pays de Loire" region.

## REFERENCES

- [1] Y. Kuang, Y. Zhang, B. Zhou, C. Li, Y. Cao, L. Li and L. Zeng, "A review of renewable energy utilization in islands," *Renewable and Sustainable Energy Reviews*, vol. 59, pp. 504-513, June 2016.
- [2] W. W. Anderson and O. A. Yakimenko, "Comparative analysis of two microgrid solutions for island green energy supply sustainability," in *Renewable Energy Research and Applications (ICRERA)*, 2017 IEEE 6th International Conference on, 2017.
- [3] M. S. H. Lipu, M. G. Hafiz, M. S. Ullah, A. Hossain and F. Y. Munia, "Design Optimization and Sensitivity Analysis of Hybrid Renewable



- Energy Systems A case of Saint Martin Island in Bangladesh," *International Journal of Renewable Energy Research (IJRER)*, vol. 7, no. 2, pp. 988-998, 2017.
- [4] J. C. Mourmouris, C. Potolias and J. G. Fantidis, "Evaluation of renewable energy sources exploitation at remote regions, using computing model and multi-criteria analysis A case-study in Samothrace, Greece," *International Journal of Renewable Energy Research (IJRER)*, vol. 2, no. 2, pp. 307-316, 2012.
  - [5] J. S. Vardakas, N. Zorba and C. V. Verikoukis, "A survey on demand response programs in smart grids: Pricing methods and optimization algorithms," *IEEE Communications Surveys & Tutorials*, vol. 17, no. 1, pp. 152-178, 2015.
  - [6] B. P. Esther and K. S. Kumar, "A survey on residential demand side management architecture, approaches, optimization models and methods," *Renewable and Sustainable Energy Reviews*, vol. 59, pp. 342-351, 2016.
  - [7] T. Logenthiran, D. Srinivasan and T. Z. Shun, "Demand side management in smart grid using heuristic optimization," *IEEE transactions on smart grid*, vol. 3, no. 3, pp. 1244-1252, 2012.
  - [8] N. U. Hassan, M. A. Pasha, C. Yuen, S. Huang and X. Wang, "Impact of scheduling flexibility on demand profile flatness and user inconvenience in residential smart grid system," *Energies*, vol. 6, no. 12, pp. 6608-6635, 2013.
  - [9] M. N. Hassanzadeh, M. Fotuhi-Firuzabad and A. Safdarian, "Wind Energy Penetration with Load Shifting from the System Well-being Viewpoint," *International Journal of Renewable Energy Research (IJRER)*, vol. 7, no. 2, pp. 977-987, 2017.
  - [10] H. J. Jabir, J. Teh, D. Ishak and H. Abunima, "Impacts of Demand-Side Management on Electrical Power Systems: A Review," *Energies*, vol. 11, no. 5, pp. 1-19, April 2018.
  - [11] K. S. Stille and J. Böcker, "Local demand response and load planning system for intelligent domestic appliances," in *Renewable Energy Research and Applications (ICRERA)*, 2015 International Conference on, 2015.
  - [12] E. Hossain, M. Z. Xahin, K. R. Islam and M. Q. Akash, "Design a novel controller for stability analysis of microgrid by managing controllable load using load shaving and load shifting techniques; and optimizing cost analysis for energy storage system," *International Journal of Renewable Energy Research (IJRER)*, vol. 6, no. 3, pp. 772-786, 2016.
  - [13] N. Smith and R. Mc Cann, "Analysis of distributed generation sources and load shedding schemes on isolated grids case study: The Bahamas," in *Renewable Energy Research and Application (ICRERA)*, 2014 International Conference on, 2014.
  - [14] N. Saker, M. Petit and J.-L. Coullon, "Demand side management of electrical water heaters and evaluation of the Cold Load Pick-Up characteristics (CLPU)," in *PowerTech*, 2011 IEEE Trondheim, 2011.
  - [15] D. Da Silva, B. Duplessis and J. Adnot, "A methodology for evaluating the energy, peak load and comfort effects of demand response control strategies for electric heating," in *ECEEE 2011 Summer Study "Energy efficiency first: The foundation of a low-carbon society"*, 2011.
  - [16] G. Strbac, "Demand side management: Benefits and challenges," *Energy Policy*, vol. 36, no. 12, pp. 4419-4426, 2008.
  - [17] A. M. Vega, D. Amaya, F. Santamaria and E. Rivas, "Energy Resource Management Integrating Generation, Load Control and Change in Consumption Habits at the Residential Level," *International Journal of Renewable Energy Research (IJRER)*, vol. 8, no. 1, pp. 101-107, 2018.
  - [18] G. Gursoy and M. Baysal, "Improved Optimal Sizing of Hybrid PV/Wind/Battery energy systems," in *Renewable Energy Research and Application (ICRERA)*, 2014 International Conference on, 2014.
  - [19] Ocean Energy Systems, "International Levelized Cost of Energy for Ocean Energy Technologies," 2015.
  - [20] D. Friedrich and G. Lavidas, "Evaluation of the effect of flexible demand and wave energy converters on the design of hybrid energy systems," *IET Renewable Power Generation*, vol. 11, no. 9, pp. 1113-1119, 2017.
  - [21] A. Bouabdallah, S. Bourguet, J. C. Olivier and M. Machmoum, "Optimal sizing of a stand-alone photovoltaic system," in *Renewable Energy Research and Applications (ICRERA)*, 2013 International Conference on, 2013.
  - [22] ECMWF, [Online]. Available: <http://www.soda-pro.com/fr/web-services/radiation/cams-radiation-service>. [Accessed 07 11 2017].
  - [23] Open Ocean SAS, "Open Ocean," 2018. [Online]. Available: [www.openocean.fr](http://www.openocean.fr). [Accessed 10 09 2018].
  - [24] V. Thapar, G. Agnihotri and V. K. Sethi, "Critical analysis of methods for mathematical modelling of wind turbines," *Renewable Energy*, vol. 36, no. 11, pp. 3166-3177, 2011.
  - [25] Enercon GMBH, "Enercon product overview," 2015.
  - [26] M. Benbouzid, J.-A. Astolfi, S. Bacha, J.-F. Charpentier, M. Machmoum, T. Maître and D. Roye, "Concepts, Modélisation et Commandes des Hydrolennes," in *Energies Marines Renouvelables*, B. Multon, Ed., Hermes Science, 2011, pp. 265-328.
  - [27] F. Lecornu, J. Paillet and H. Ravenel, "PREVIMER – Coastal Observations & Forecasts - Summary of 2 years demonstration and future perspectives," in *SeaTechWeek 2008, Coastal Operational Oceanography*, 2008.
  - [28] D. Silva, E. Rusu and C. G. Soares, "Evaluation of Various Technologies for Wave Energy Conversion in the Portuguese Nearshore," *Energies*, vol. 6, no. 3, pp. 1344-1364, 2013.
  - [29] E. Boudière, C. Maisondieu, F. Ardhuin, M. Accensi, L. Pineau-Guillou and J. Lepasqueur, "A suitable metocean hindcast database for the design of Marine energy converters," *International Journal of Marine Energy*, Vols. 3-4, pp. 40-52, Décembre 2013.
  - [30] B. Bhandari, K.-T. Lee, G.-Y. Lee, Y.-M. Cho and S.-H. Ahn, "Optimization of hybrid renewable energy power systems: A review," *International journal of precision engineering and manufacturing-green technology*, vol. 2, no. 1, pp. 99-112, 2015.
  - [31] R. Rigo-Mariani, "Méthodes de conception intégrée "dimensionnement-gestion" par optimisation d'un micro-réseau avec stockage," Thèse de Doctorat, Institut National Polytechnique de Toulouse, 2014.
  - [32] EDF SEI, March 2018. [Online]. Available: <https://opendata-iles-ponant.edf.fr/explore/dataset/conso-3-iles-final/>. [Accessed 20 Mars 2018].
  - [33] Les îles du Ponant, «Les îles du Finistère : Lancement opérationnel de la transition énergétique,» 2017.
  - [34] Ö. Özkizilkaya, "Thermosensibilité de la demande électrique : identification de la part non linéaire par couplage d'une modélisation bottom-up et de l'approche bayésienne," 2014.
  - [35] ADEME, «Coûts des énergies renouvelables en France,» 2016.
  - [36] A. Saez de Ibarra Martinez De Contrasta, "Optimal sizing and control of energy storage systems for the electricity markets participation of intelligent photovoltaic power plants," 2016.
  - [37] IRENA, "Electricity storage and renewables: Costs and markets to 2030," 2017.
  - [38] P. Gardner, F. Jones, M. Rowe, A. Nouri and H. Van de Vegte, "E-storage: Shifting from cost to value: Wind and solar applications," 2016.